ANALYTICAL STUDY OF VORTEX FLAPS ON HIGHLY SWEPT DELTA WINGS

Neal T. Frink
Aeronautical Engineer
NASA Langley Research Center
Hampton, Virginia USA

Abstract

This paper highlights some current results from ongoing analytical studies of vortex flaps on highly swept delta wings. A brief discussion of the vortex flow analysis tools is given along with comparisons of the theories to vortex flap force and pressure data. Theoretical trends in surface pressure distribution for both angle-of-attack variation and flap deflection are correctly predicted by Free Vortex Sheet theory. Also shown are some interesting calculations for attached-flow and vortex-flow flap hinge moments that indicate flaps utilizing vortex flow may generate less hinge moment than attached flow flaps. Finally, trailing-edge flap effects on leading-edge flap thrust potential are investigated and theory-experiment comparisons made.

Nomenclature

AR	aspect ratio, b^2/S_{ref}
b	span
C_D	drag coefficient, drag/$q_\infty S_{ref}$
$C_{D,o}$	zero lift drag coefficient, clean configuration
ΔC_{D_p}	profile drag, $C_D-(C_L^2/\pi AR)$
C_H	hinge moment coefficient, hinge moment/$q_\infty S_f \bar{c}_f$
C_L	lift coefficient, lift/$q_\infty S_{ref}$
C_m	pitching moment coefficient, pitching moment/$q_\infty S_{ref} \bar{c}$
C_p	pressure coefficient, $(p-p_\infty)/q_\infty$
$\bar{c}$	reference chord
c_r	root chord
FVS	free vortex sheet
L/D	lift-to-drag ratio
L/W	load factor, lift/weight
M_H	hinge moment
M	Mach number
p	static pressure
q	dynamic pressure, $\rho V^2/2$
S	area
s	local semispan
V	velocity
VLM-SA	vortex lattice method--suction analogy
QVLM-SF	quasi-vortex lattice method--separated flow
x	cartesian coordinate, positive downstream
y	cartesian coordinate, positive starboard
z	cartesian coordinate, positive up
α	angle of attack, degrees
δ	flap deflection angle in plane normal to hinge line, positive downward, degrees
η_h	$(b/2)_h/(b/2)$
Λ_{LE}	leading-edge sweep angle, degrees
Λ_h	hinge-line sweep angle, degrees
ρ	density

Subscripts

f	flap
h	hinge line
LE	leading edge
ref	reference
TE	trailing edge
u	upper
δ	flap deflection
∞	freestream reference

Introduction

The complexity of tactical aircraft mission requirements generally increases in proportion to that of the perceived threat. Consequently, for both tactical and economic reasons, each new generation of combat aircraft is being forced to fulfill more milti-mission roles than its predecessors. Current perceptions of the near-term threat indicate a need for future fighter aircraft to have efficient sustained supersonic cruise performance coupled with a transonic maneuver capability similar to that of the current lightweight fighters[1]. The technology for

accomplishing these objectives is available in concept but must be matured before configurational application is possible.

Coupling the two requirements for supersonic cruise and transonic maneuver into one aircraft presents a dichotomy in design logic. On the one hand, a supersonic cruise requirement drives the configuration toward a highly swept, low-aspect ratio, slender wing planform with low wing loading. Conversely, the transonic maneuver condition is generally achieved through a relatively higher aspect ratio wing and a higher wing loading. Within the limitations of current engine technology, the primary driver for the subject aircraft design is its supersonic cruise element, thus, its planform will most likely be slender. The problem associated with meeting these dual requirements is illustrated in figure 1. This figure portrays the untrimmed maneuver lift-to-drag efficiency as a function of load factor for a current transonic fighter[2] and a proposed supersonic cruise fighter with both fixed and variable geometry[3] at M_∞ = 0.85 and 9144 meters (30 000 feet). The assumed wing loadings are 3016 N/m^2 (63 lb/ft^2) for the transonic fighter and 1915 N/m^2 (40 lb/ft^2) for the supersonic cruise fighter. As can be seen, the transonic maneuver performance for the slender wing fixed geometry is significantly below that for the transonic fighter. The reason for this difference is that slender wing geometries operating at moderate to high angle-of-attack conditions develop a stable separation induced vortex flow which generates significant lift increments along with a substantial drag penalty associated with the loss of leading-edge suction. While the high lift is advantageous for instantaneous maneuvering, the boundaries of the sustained maneuver envelope are dictated to a large extent by the available thrust. Thus, it is imperative that the drag associated with large load factors be reduced as much as possible. As can also be seen in figure 1, some lift-to-drag improvement is possible on the supersonic cruise configuration by deflecting simple variable leading- and trailing-edge flaps on a planar wing. It was demonstrated in reference 4 that this variable geometry supersonic cruise configuration achieves nearly the same supersonic cruise performance as its optimum supersonic camber design.

The concept of using variable leading-edge geometry as a solution to the slender wing drag problem is generally applied in two manners; 1) suppress the formation of leading-edge vortices through proper matching of a smooth, continuously warped leading edge to the local upwash so as to promote attached flow conditions[5], and 2) waive the leading-edge attachment condition and permit the flow to separate forming a controlled stable leading-edge vortex along a forward facing cambered surface[3]. The first solution should have some application to vehicles operating within a moderate lift range, but seems impractical in the combat environment where high maneuver load factors make it extremely difficult to maintain completely attached flow. Furthermore, assuming the flow remains attached along the leading edge at the large lift increments of interest, the required leading-edge deflection is so severe that separation downstream of the "hinge line" cannot be avoided[6]. The second approach seeks to use the naturally ocurring vortex flow advantageously both for recovering lost leading-edge suction and for promoting attached flow aft of the hinge line. The configuration described in reference 3 is typical of supercruiser class planforms and was designed to beneficially utilize vortex flow for achieving drag levels at a maneuver lift coefficient comparable to those theoretically attainable through optimal camber for attached flow. Of equal significance was a further demonstration[3] that levels of effective thrust recovery comparable to those attained by near optimal cambering could be realized by deflecting certain combinations of simple leading- and trailing-edge flaps on a planar wing of the same planform. This is a very attractive result from a practical design and fabrication standpoint. These results led to further exploratory wind-tunnel tests[7] of the simple leading-edge flap concept which was thereafter termed the "vortex flap." Additional vortex flap related experimental studies are reported in references 8 to 12. The vortex flap concept along with a scope of the current overall vortex flap analysis capability is illustrated in figure 2. This figure shows the concept applied to a 74^o wing-body pressure model which in turn is modeled theoretically and the results compared.

In addition to improving transonic maneuver performance, vortex flaps offer some other potential advantages. They are: 1) an upward flap deflection can be used for landing to generate the needed high lift and high drag[13], 2) large downward deflections at touchdown to generate negative lift and high drag could possibly be used in place of a drag chute[13], 3) vortex flaps benefit from sharp edges which may be important in low observable technology, and 4) asymmetric vortex flap deflections may generate sufficient rolling and yawing moments to be useful for high angle-of-attack lateral control[9].

Currently, NASA Langley Research Center is involved in an aggressive experimental and theoretical effort to mature the vortex flap technology to the point of practical application. The purpose of the present paper is to highlight some results from recent theoretical application studies of vortex flaps, including the effects of angle of attack and flap deflection angle on upper surface pressure distributions, and forces and moments. Also of interest is a comparison between vortex flow and attached flow flap hinge moments. Finally, trailing-edge flap effects on leading-edge flap thrust potential are investigated and theory-experiment comparisons made.

Vortex Flow Analysis Tools

Three analytical methods currently available to the author for calculating vortex flow aerodynamics will be briefly described herein. The methods differ greatly in the extent of detail to which the vortex flow field is modeled and in the cost of computation. Each method, illustrated in figure 3, will be described in the order of increasing analytical sophistication.

VLM-SA

The Vortex Lattice Method with Suction Analogy (VLM-SA)[14] is a simple, inexpensive method that has been used extensively for the estimation of total aerodynamic vortex-induced forces and moments on slender wings. The method was further extended by Lamar[15] to accommodate camber and twist. This extended VLM-SA calculates the potential flow leading-edge suction for the cambered and twisted wing in a planar computational plane and then applies preliminary corrections to account for the warped surface orientation. The leading-edge suction vector is rotated normal to the warped surface at the leading edge, as prescribed by the suction analogy (see fig. 3), to arrive at the contributions to lift, drag, and pitching moment. These contributions are then added to the potential flow results to form the total vortex-induced aerodynamic coefficients. The method satisfies the trailing-edge Kutta condition but only approximates the effect of the leading-edge Kutta condition by the suction analogy. Hence, this method can only estimate forces and moments and not the vortex-induced surface pressure distributions. The extended VLM-SA was used in the design reported in reference 3.

QVLM-SF

The quasi-vortex lattice method for separated flow (QVLM-SF)[16] is one of intermediate sophistication to the VLM-SA and to higher order panel methods such as the Free Vortex Sheet Theory to be discussed in the next section. It contains the capability of calculating distributed loads and total aerodynamic characteristics for low-aspect-ratio wings, but not surface pressures. The method models the wing potential flow by distributing a quasi-vortex lattice (i.e., the continuous chordwise loads are represented by a series of discrete elements) on a planar-solution surface accounting for camber and twist in the boundary conditions. To model the separated leading-edge vortex flow, discrete filaments of vorticity are attached to the leading edge of the planar-solution surface as shown in figure 3. The strengths and essential force free locations of these vortex filaments, which are composed of a series of straight line segments, are determined in conjunction with the QVLM wing solution by iteration.

FVS

The Free Vortex Sheet (FVS) theory[17,18] which represents one of the more thorough formulations to date, is a fully three-dimensional, inviscid, potential flow formulation which models steady subsonic flow about wings or wing-body configurations with separation-induced leading- and/or side-edge vortex flow. The separation line is assumed known which, for the configurations of interest, is along the sharp leading edges. Quadratic doublet panels are used to model thin wings, wakes, and vortex networks while linear source panels are used to model thickness effects such as fuselages (fig. 3). Since the geometry and doublet strengths of the free- and fed-sheets are not known in advance, they must be determined iteratively in the presence of the cambered wing. The solution is said to have converged when the boundary conditions of no flow through the wing, no flow through and zero pressure jump across the free sheet, no force on the fed sheet, and zero pressure jump across the near wake are satisfied to within a stipulated global tolerance. The Kutta condition is satisfied along all edges with this formulation. A more thorough description of the theory along with application to a range of configurations including vortex flapped ones are given in reference 19. Other application studies using the FVS theory for both planar and cambered wings are described in references 20 to 24.

Validation of Theories

Before proceeding with the analytical vortex flap study, the subject theories are verified with experimental data to establish a level of confidence in the results. The selected experimental data are unpublished and were obtained in the NASA Langley Research Center 7- by 10-Foot High-Speed Tunnel, by Dr. D. M. Rao, on a 74° delta wing-body pressure model fitted with a constant chord vortex flap (see fig. 2). For the present study, comparisons are only made with the VLM-SA and FVS theories, since reference 3 indicated that the QVLM-SF yields unsatisfactory results for delta wings with large leading-edge cambers.

Forces and Moments

Figure 4 presents a comparison of force and moment coefficients between experimental data and the VLM-SA and FVS theories. The results are shown at an $\alpha = 14^{\circ}$ and $M_{\infty} = 0.3$ so as to summarize the effect of flap deflection on the coefficients. Note in the sketch on the right of figure 4 that there are differences in the experimental and theoretical geometries. In particular, the geometry used for the theoretical calculations is a wing alone configuration where the cylindrical fuselage has been omitted and the wing extended into the centerline. Also note that there is additional area in the apex region of the flap on the theoretical geometry. (Because of these differences in geometry, a common reference area comprised of the wing planform area extending into the centerline but excluding the flap area was used in force and moment calculations.) These modifications were necessary to obtain solution convergence in the FVS code, which yielded converged solutions at $\alpha = 14^{\circ}$ for flap deflections up to 20°. Quantitatively, the two theories are showing an overestimation of lift and drag for flap deflections from 0° to 30° measured normal to the hinge line. These overestimations initially are surprising because the VLM-SA generally underpredicts drag on cambered configurations since the suction analogy prescribes the rotated suction vector to be applied at the leading edge[25]. However, the excellent qualitative correlation of lift and drag suggests the differences may be a result of the variance in geometry. The moment coefficients are not estimated as well as the forces but the FVS theory exhibits the qualitative behavior of the data.

Pressures

A correlation of experimental and FVS theoretical pressures for the same configuration described in figure 4 is shown in figure 5. The spanwise upper surface pressures at the chord

station indicated on the sketch are shown in figure 5 for flap deflections of 0^o, 10^o, and 20^o The spanwise coordinate is nondimensionalized by the local hinge semispan, $(s)_h$, so that pressures acting on the flap surface correspond to $y/(s)_h > 1$ and on the wing surface to $y/(s)_h < 1$. As can be seen, pressures are estimated quite well by the FVS theory, particularly for deflections of 0^o and 10^o. For $\delta_{LE} = 20^o$, the theory overpredicts the suction peak but its general spanwise position is in good agreement with the data. Over the range of deflections presented, the general character of the data is preserved by the theory. Both theory and experiment exhibit an outward shift in suction peak location and a corresponding rise in peak level with increasing flap deflection along with a decrease in suction just inboard of the hinge line. It should be noted that secondary vortex effects are not modeled by the FVS theory which is the reason for the underprediction of pressures over the outboard region of the flap.

With a certain degree of confidence in the theories now established, the ensuing analytical study may proceed.

Conical Flap Study

The present analytical study is one of many systematic steps being taken toward practical application of vortex flaps. One of the uncertainties regarding the application of vortex flaps is whether the hinge moments will be sufficiently large to present structural and flap actuation problems. The following analysis attempts to address this question from a theoretical standpoint.

In reference 19, a systematic series of vortex flap configurations were analyzed to identify aerodynamic trends associated with the variation of pertinent geometric parameters. That study was performed on a 74^o delta wing at $M_\infty = 0$ using the FVS theory where the leading edge flap was sharp and deflected about a hinge line emanating conically from the apex. The primary variables studied in reference 19 were flap deflection, hinge-line position, and angle of attack. The present paper will further analyze the results of the parametric conical vortex flap series by examining the vortex flow hinge moments in relation to their attached flow hinge moments. Since hinge moments are generated by distributions of pressures on the cantilevered flap, the sensitivity of pressures to angle of attack will be examined first.

Pressure Distribution with α

The sensitivities of vortex core position and pressure distribution to angle of attack are shown in figure 6 for the $\eta_h = 0.7$ configuration with $\delta_{LE} = 20^o$. The hinge-line position, η_h, is defined as the ratio of hinge semispan to total undeflected semispan. This figure depicts upper-surface pressure distributions and respective core locations at the 44-percent chord station relative to the subject crossplane geometry, which is nondimensionalized by the local semispan of the undeflected wing. All flap deflections are measured normal to the hinge line, and the presented results are characteristic of those manifested along the entire chordwise extent of the wing.

In figure 6, the expected effects are a substantial inward and upward shift in core position along with a related inboard movement of the suction peak as angle of attack increases from 11^o to 20^o. At $\alpha = 13^o$ the suction peak occurs over the hinge line, so that at lower α's the peak is over the flap and at higher α's the peak is over the wing. From this, one might anticipate that flap hinge moments will decrease with increasing angle of attack, hence C_L, which is opposite to that expected for attached flow. Hinge moments will be examined more explicitly in the next section.

Hinge Moments

Flow type. Figure 7 shows the effect of flow type (vortex flow versus attached flow) on the theoretical flap hinge moment variation with lift coefficient for the same geometry used in figure 6. All estimates of hinge moment, both attached flow and vortex flow, were extracted from FVS calculations. (In addition to solving leading-edge vortex problems, the FVS code can also be used in an attached flow mode, which is done for the present results.) The reference area and chord, S_f and $\bar{c}_f$, are defined as the flap surface area and the semispan of the undeflected flap at the trailing edge, respectively. Small insets of representative upper surface pressure distributions relative to their crossplane geometry at $x/c_r = 0.44$ are provided to aid in interpretation of the hinge moments. The most unusual result evident on figure 7 is that the attached flow moments are overall higher than those for vortex flow. This result was not expected but is reasonable considering an attached flow slender wing configuration requires a higher α to achieve a desired C_L than does a vortex flow configuration. The reason for these differences in moment is evident from the pressure insets which show the attached flow leading-edge singularity acting over a longer moment arm than the vortex-induced suction pressures. As expected, vortex-flow hinge moments decrease and attached-flow moments increase as C_L increases. These trends correlate with the inboard movement of the vortex-induced suction peak with increasing C_L and the corresponding increase in attached-flow leading-edge singularity strength.

It is recognized that the attached flow pressure distributions shown on figure 7 are not totally realistic. In fact, for the fixed geometry under consideration, the real flow will not remain attached, but will separate at the leading edge and form a stable vortex system. If a smooth onflow condition is pursued by adding more flap deflection and twist as was done in reference 5, the leading-edge singularity would be alleviated and the hinge moment reduced. However, as previously mentioned, separation at the flap knee cannot be avoided at the higher lift coefficients. Evidence of this problem is seen in the attached-flow pressure curves of figure 7 as a small suction "bump" over the hinge line where the flow

must negotiate the corner. Rounding of the knee will offer some relief to the strong pressure gradients there, but this alone is not enough to solve the separation problem as demonstrated in reference 6.

Flap deflection. The impact of flap deflection on theoretical hinge moment is presented in figure 8 for the configuration at $C_L = 0.4$. These calculations for the vortex flow were performed at $\alpha = 14^o$, hence the corresponding C_L actually decreases slightly with increasing δ_{LE}. The values for C_L however are within the single digit accuracy specified. The related attached flow C_L's were matched to those for the vortex flow. The results show that, once again, the attached flow hinge moments are larger than those for vortex flow. It is noted that the effect of increasing flap deflection is to decrease the local upwash relative to the leading edge. Hence, for vortex flow, the vortex should decrease in size and reside more outboard over the flap along with its consequent suction peak. By following this reasoning, the hinge moment should increase with increasing flap deflection as is indeed the case in figure 8. Similarly, the attached flow leading-edge singularity strength should diminish and result in a consequent hinge moment decrease.

Hinge line. Figure 9 shows the effect of conical hinge line position, η_h, on theoretical flap hinge moment for the configuration at $C_L = 0.5$ and with $\delta_{LE} = 20^o$. As in the previous two figures, the attached flow hinge moments are overall larger than the vortex flow moments. The moments for the two flow fields are relatively close in value for the larger flaps (smaller η_h) but diverge as flap size is decreased (increasing η_h). The reason for this decrease in vortex-flow hinge moment is evident from the pressure distributions. The cause for the increase in attached-flow moment with decreasing flap size is more subtle. It would appear that, for a constant lift coefficient and similar levels of pressure associated with the leading-edge singularity, the larger flap would generate the larger hinge moment since it has a longer moment arm. The larger flap may in fact generate larger attached-flow hinge moments. In the definition for the hinge moment coefficient

$$C_H = \frac{M_H}{q_\infty S_f \bar{c}_f}$$

S_f and $\bar{c}_f$ are functions of hinge line position (flap size). Therefore, small values for the reference flap area and chord, S_f and $\bar{c}_f$, respectively, will tend to increase C_H unless M_H decreases by a comparable amount. For comparative purposes, however, the moment coefficients were calculated for the two flow fields in a consistent manner.

The preceding hinge moment analysis was not presented to establish that vortex flaps are necessarily better than the attached-flow flaps. All theoretical limitations are recognized. The intent of the analysis was to stimulate current thinking regarding the practicality of vortex flaps. In short, the results suggest that vortex flaps may present no more of a loads and actuation problem for an aircraft systems design than an attached-flow flap.

Constant Chord Flap

The remaining section will highlight several features related to the theoretical formulation and performance of a constant chord vortex-flap configuration. In particular, a simple input geometry will be identified which yields FVS pressure distributions very close to those measured on a more complex wing-body configuration, thus saving considerable computer resources. Then, hinge moment calculations for the constant chord vortex flap will be presented followed by a discussion of trailing-edge flap effects on vortex flap performance.

Theoretical Formulation

The FVS code is generally considered an expensive program to run. For this reason, there is an ongoing effort to discover ways to obtain converged solutions from the theory at lower cost. Some of the ideas pursued in reference 19 involve code modification and cleverness on the part of the user to generate a better starting solution. Another approach proposed herein comprises actual modification to the configurational geometry to make it more amenable to FVS solution convergence while at the same time reducing the number of required panels.

Figure 10 shows the pressure distributions at two chord stations for two formulations of a 74^o delta wing-vortex flap configuration at $\alpha = 14^o$ with $\delta_{LE} = 10^o$. The part-span formulation illustrated by the right half of the geometry sketch inset is characterized by the constant chord vortex flap being attached to the wing hinge line only part way along the wing leading edge. This is the same wing-alone formulation used in figures 4 and 5 which yielded good agreement with the wing-body configuration data. The modified formulation, which is illustrated by the dashed geometry shown in the left half of the geometry inset, was derived from the part-span formulation by removing the portion of wing inboard of the apex of the flap and then joining the new geometry at the centerline to form a full-span flap configuration. The true flap area remains the same but the ratio of flap to total area is increased by the modification. As can be seen in figure 10 by the spanwise pressure distributions at chord stations $x/c_r = 0.59$ and 0.74, agreement is good both quantitatively and in nondimensional spanwise location of pressure values. The full-span flap results shown in figure 10 required approximately two-thirds the computer resources needed for the part-span solution.

Problems do occur in using the simpler configuration when making comparisons of total force and moment coefficients between the two

formulations because the geometries are completely different in a nondimensionalized sense. However, if one is iteratively designing a vortex flap by monitoring the effect of geometrical perturbations on upper surface pressure distribution, then the simpler formulation should suffice.

Hinge Moment

In line with the conical flap study discussed in a previous section, it is desirable to obtain the effect of flow type on the theoretical hinge moments for the constant chord flap as well. Figure 11 shows the calculated attached-flow and vortex-flow hinge moments for the part span flap configuration at $C_L \approx 0.55$ over a deflection range from 0^o to 20^o. The trends are similar to those exhibited by the conical flap in figure 8, but the magnitude of coefficients for the constant chord flap are more than double that for the conical flap. The primary reason for this difference is that the reference chord, $\bar{c}_f$, is defined as the flap semispan at the trailing edge instead of the average flap chord. For the conical geometry, the average flap chord is approximately half the flap trailing edge semispan and would increase the coefficient values by a factor of two.

Trailing Edge Flap Effects

It has been demonstrated in reference 9 that trailing-edge flaps induce an additional increment of reduced drag on highly swept delta wings when applied in conjunction with leading-edge vortex flaps. In this final section, trailing edge flap effects are explored both analytically and experimentally for the 74^o delta wing-body configuration having constant chord vortex flaps. The prescribed theoretical and experimental geometries are discernible in the sketch on figure 12 and are the same used in the preceding theory-experiment comparisons of figures 4 and 5 with the exception of the trailing edge flap. Figure 12 shows the effect of leading- and trailing-edge flap deflection on profile drag, ΔC_{D_p}, which is defined as $C_D - (C_L^2/\pi AR)$. An experimental value of 0.0104 for $C_{D,o}$ was added to the theoretical results. The data and theory both show the expected further drag reduction at the higher lift coefficients promoted by the trailing-edge flap. The theory, however, generally underpredicts the data, but this is not surprising because of the basic small vortex assumption of the suction analogy. The primary mechanism leading to the additional drag reduction associated with the trailing-edge flap is a decrease in angle of attack for a given lift coefficient which results in a net drag reduction. The lower angle of attack in turn orients the vortex flap surface in a more forward facing direction thus increasing its thrust potential at the higher lift coefficients. Further benefits are realized from the trailing-edge flap at low angles of attack in the form of increased circulation, hence, upwash at the leading edge, which enhances the vortex flap thrust potential. The favorable effects from the trailing edge flaps are significant with regard to practical application since they are used to provide trim for delta wings.

Concluding Remarks

An analytical study of vortex flaps on highly swept delta wings has been presented highlighting some of the practical features of the device. A reasonable degree of confidence in the analysis theories has been established through correlations with both force and pressure data. Trends in surface pressure distribution for both angle of attack variation and flap deflection are correctly predicted by the Free Vortex Sheet theory. A comparative study between vortex and attached flow flaps revealed that vortex flaps generate less theoretical hinge moment at constant lift than the same flap operating under assumed attached-flow conditions. This result suggests that vortex flaps may present no more of a loads and actuation problem than an attached-flow flap. Since the Free Vortex Sheet theory is expensive to operate, a simple geometrical representation for approximating a more complex delta wing-body configuration is proposed and shown to be satisfactory for calculating the surface pressure distribution. Finally, it was shown that deflecting the trailing-edge flap further reduced drag compared to that obtained with leading-edge flap alone, and that these trends are correctly exemplified by the vortex lattice method--suction analogy, though the quantitative drag values are underpredicted by theory due to basic assumptions of the suction analogy.

References

[1]Barlow, R. C.; Collier, K. I.; and Richey, G. K.: Military Aircraft Technology: Needs and Trends for the 80's. AIAA Paper No. 81-1691, Dayton, Ohio, August 11-13, 1981.

[2]Webb, J. B., et. al.: F-16 Aerodynamic Design Data Report CDRL Sequence No. A027, General Dynamics Fort Worth Report No. 16PR177 (Contract F33657-75-C-0310), Revised November 1976.

[3]Lamar, J. E.; Schemensky, R. T.; and Reddy, C. S.: Development of a Vortex-Lift Design Procedure and Application to a Slender-Maneuver Wing Configuration. AIAA Paper No. 80-0327R, Journal of Aircraft, Vol. 18, No. 4, pp. 259-266, April 1981.

[4]Miller, D. S.; and Schemensky, R. T.: Design Study Results of a Supersonic Cruise Fighter Wing. AIAA Paper No. 79-0062, New Orleans, Louisiana, January 15-17, 1979.

[5]Coe, P. L.; Huffman, J. K.; and Fenbert, J. W.: Leading-Edge Deflection Optimization for a Highly Swept Arrow-Wing Configuration. NASA TP-1777, 1980.

[6]Schoonover, W. E., Jr.; and Ohlson, W. E.: Wind-Tunnel Investigation of Vortex Flaps on a Highly Swept Interceptor Configuration. ICAS-82-6.7.3, August 1982.

[7]Rao, D. M: Leading-Edge Vortex Flap Experiments on a 74-Deg Delta Wing. NASA CR-159161, 1979.

[8]Rao, D. M.: Exploratory Subsonic Investigation of Vortex-Flap Concept on Arrow Wing Configuration. NASA CP-2108, (Part I), pp. 117-129, 1979.

[9]Rao, D. M.: Leading-Edge 'Vortex Flaps' for Enhanced Subsonic Aerodynamics of Slender Wings. ICAS-80-13.5, pp. 554-562, October 1980.

[10]Marchman, J. F., III: Effectiveness of Leading-Edge Vortex Flaps on 60 and 75 Degree Delta Wings. Journal of Aircraft, Vol. 18, No. 4, pp. 280-286, April 1981.

[11]Yip, L. P.; and Murri, D. G.: Effects of Vortex Flaps on Low-Speed Aerodynamic Characteristics of an Arrow Wing. NASA TP-1914, 1981.

[12]Rao, D. M.: Upper Vortex Flap--A Versatile Surface for Highly Swept Wings. ICAS-82-6.7.1, August 1982.

[13]Tingas, S. A.; and Rao, D. M.: Subsonic Balance and Pressure Investigation of a 60° Delta Wing with Leading-Edge Devices. NASA CR-165923, June 1982.

[14]Lamar, J. E.; and Gloss, B. B.: Subsonic Aerodynamic Characteristics of Interacting Lifting Surfaces with Separated Flow Around Sharp Edges Predicted by a Vortex Lattice Method. NASA TN D-7921, 1975.

[15]Lamar, J. E.; and Herbert, H. E.: Prediction Version of the Extended NASA-Langley Vortex Lattice FORTRAN Computer Program--Volume I--User's Guide. NASA TM-83303, April 1982.

[16]Mehrotra, S. C.; and Lan, C. E.: A Theoretical Investigation of the Aerodynamics of Low-Aspect-Ratio Wings with Partial Leading-Edge Separation. NASA CR-145304, 1978.

[17]Johnson, F. T.; Lu, P.; Tinoco, E. N.; and Epton, M. A.: An Improved Panel Method for the Solution of Three-Dimensional Leading-Edge Vortex Flows. Volume I--Theory Document. NASA CR-3273, July 1980.

[18]Tinoco, E. N.; Lu, P.; and Johnson, F. T.: An Improved Panel Method for the Solution of Three-Dimensional Leading-Edge Vortex Flows. Volume II--User's Guide and Programmer's Document. NASA CR-3279, July 1980.

[19]Luckring, J. M.; Schoonover, W. E., Jr.; and Frink, N. T.: Recent Advances in Applying Free Vortex Sheet Theory for the Estimation of Vortex Flow Aerodynamics. AIAA Paper No. 82-0095, Orlando, Florida, January 11-14, 1982.

[20]Tinoco, E. N.; and Yoshihara, H.: Subcritical Drag Minimization for Highly Swept Wings with Leading-Edge Vortices. AGARD CP-247, Paper No. 26, January 1979.

[21]Lamar, J. E.; and Luckring, J. M.: Recent Theoretical Developments and Experimental Studies Pertinent to Vortex Flow Aerodynamics--With a View Towards Design. AGARD CP-247, Paper No. 24, January 1979.

[22]Kuhlman, J. M.: Analytical Studies of Separated Vortex Flow on Highly Swept Wings. NASA CR-3022, 1978.

[23]Johnson, F. T.; and Tinoco, E. N.: Recent Advances in the Solution of Three-Dimensional Flows Over Wings with Leading-Edge Vortex Separation. AIAA Paper No. 79-0282, New Orleans, Louisiana, January 15-17, 1979.

[24]Reddi, C. S.: Investigation of Aerodynamic Characteristics of Wings Having Vortex Flow Using Different Numerical Codes. NASA CR-165706, 1981.

[25]Lan, C. E.; and Chang, J. F.: Calculation of Vortex Lift for Cambered Wings by the Suction Analogy. NASA CR-3449, 1981.

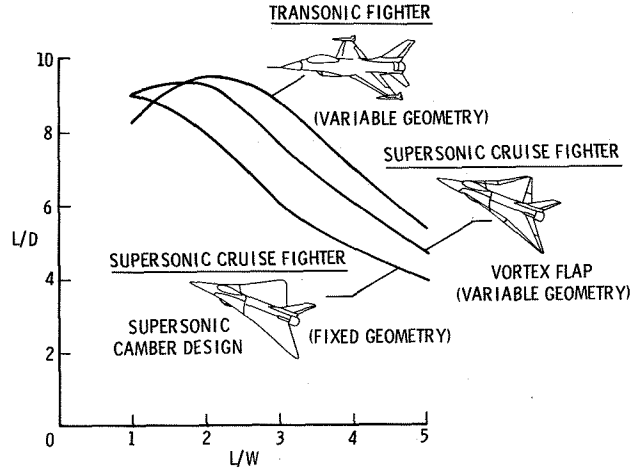

Figure 1. Transonic Maneuver Performance. M_∞ = 0.85, 9144 meters (30 000 ft) altitude.

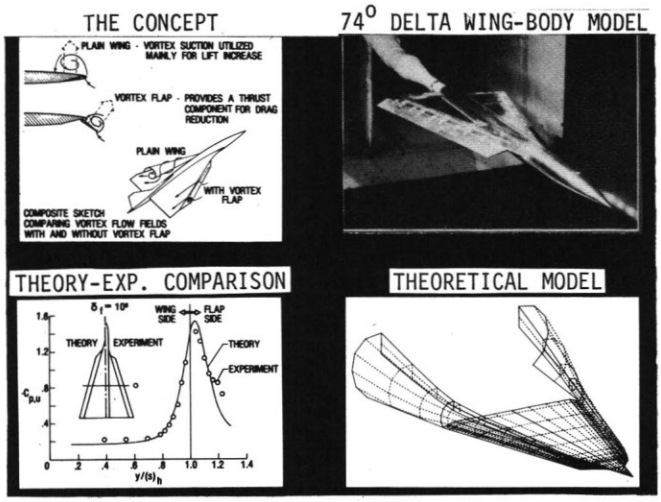

Figure 2. Vortex Flap Analysis Capability.

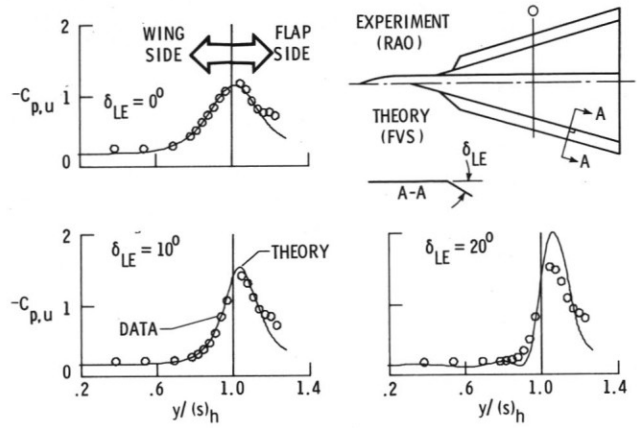

Figure 5. Effect of Flap Deflection on Spanwise Pressure Distribution. $\Lambda_h = 74^o$, $\alpha = 14^o$, $M_\infty = 0.3$.

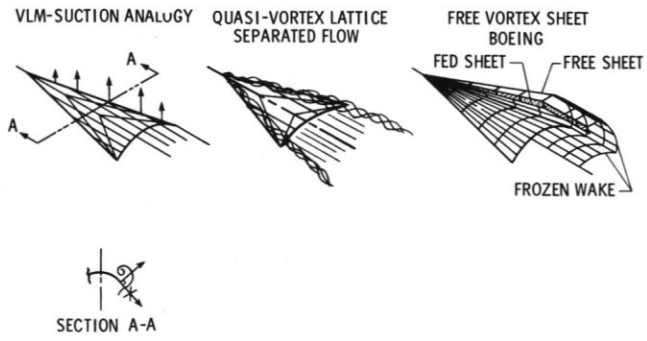

Figure 3. Vortex Flow Aerodynamic Representation.

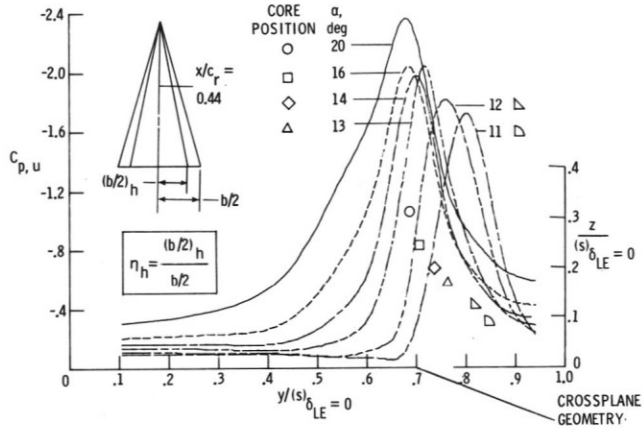

Figure 6. Theoretical Sensitivity of Wing Pressure and Core Location to Angle of Attack. $\Lambda_{LE} = 74^o$, $\eta_h = 0.7$, $\delta_{LE} = 20^o$, $M_\infty = 0$.

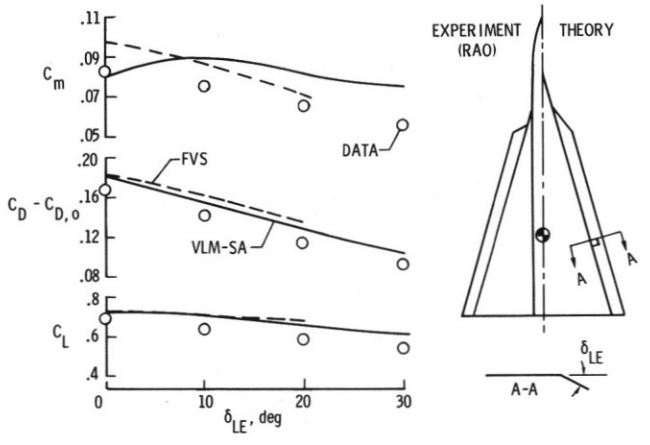

Figure 4. Effect of Flap Deflection on Force and Moment Coefficients. $\Lambda_h = 74^o$, $\alpha = 14^o$, $M_\infty = 0.3$.

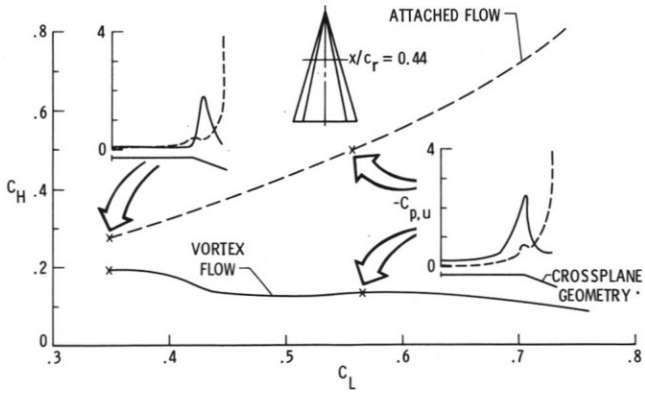

Figure 7. Effect of Flow Type on Theoretical Flap Hinge Moment, Vortex Versus Attached Flow, Conical Flap. $\Lambda_{LE} = 74^o$, $\eta_h = 0.7$, $\delta_{LE} = 20^o$, $M_\infty = 0$.

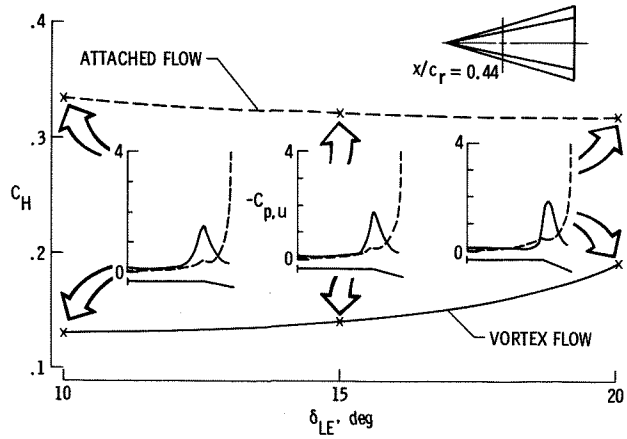

Figure 8. Effect of Flap Deflection on Theoretical Hinge Moment, Conical Flap. $\Lambda_{LE} = 74^{o}$, $\eta_h = 0.7$, $C_L = 0.4$, $M_\infty = 0$.

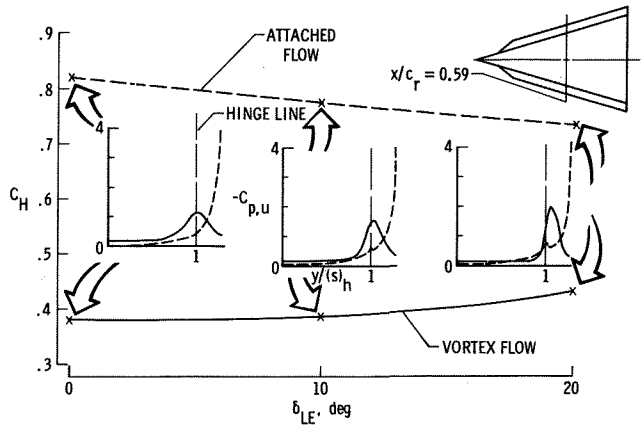

Figure 11. Effect of Flap Deflection on Theoretical Hinge Moment, Constant Chord Flap. $\Lambda_h = 74^{o}$, $C_L \approx 0.55$, $M_\infty = 0$.

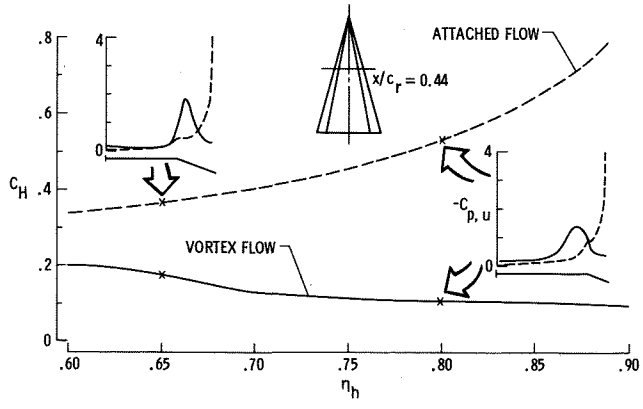

Figure 9. Hinge Line Effect on Theoretical Flap Hinge Moment, Conical Flap. $\Lambda_{LE} = 74^{o}$, $\delta_{LE} = 20^{o}$, $C_L = 0.5$, $M_\infty = 0$.

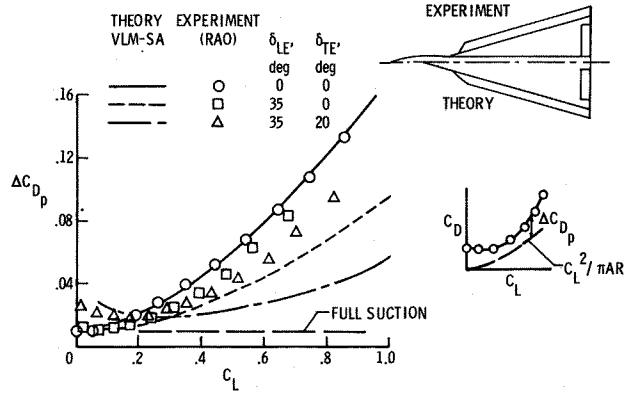

Figure 12. Effect of Flap Deflection on Profile Drag. $M_\infty = 0.3$.

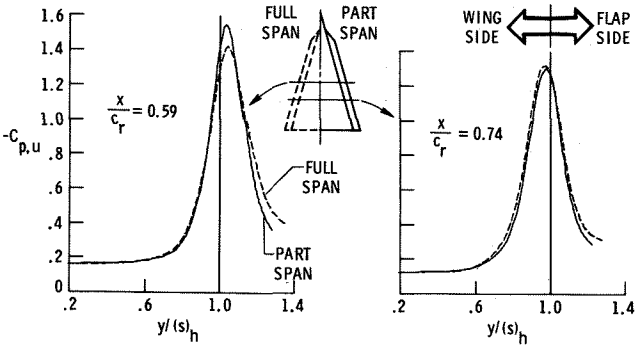

Figure 10. Effect of Part-Span Versus Full-Span Formulation on FVS Pressures. $\Lambda_h = 74^{o}$, $\alpha = 14^{o}$, $\delta_{LE} = 10^{o}$, $M_\infty = 0$.